ELSEVIER

Journal of Alloys and Compounds 279 (1998) 70–74

Journal of ALLOYS AND COMPOUNDS

Toward multiscale modelling: the role of atomistic simulations in the analysis of Si and SiC under hydrostatic compression

Kazuki Mizushima[a,*], Meijie Tang[1,b], Sidney Yip[b]

[a]*Central Research Institute, Mitsubishi Materials Corporation, 1-297 Kitabukuro-cho, Omiya, Saitama 330, Japan*
[b]*Department of Nuclear Engineering, Massachusetts Institute of Technology, Cambridge, MA 02139, USA*

Abstract

The structural responses of silicon and silicon carbide under hydrostatic compression have been analyzed by using Tersoff interatomic potential function. We show the elastic stability criteria, based on the elastic stiffness coefficients gives consistent predictions of critical pressures at which the lattices become unstable with molecular dynamics simulations. However, the predicted values are considerably higher than that of another prediction based on the thermodynamic criteria. By calculating activation barriers for the homogeneous silicon phase transition from cubic diamond to β-Sn, we suggest that the elastic and thermodynamic criteria give upper and lower bounds respectively on the transition pressure. We also show that the effect of the atomic size disparity between Si and C atoms can be dominant in favoring amorphization over polymorphic transition in silicon carbide.

Keywords: Materials design; Molecular dynamics; Pressure; Phase transition; Silicon; Silicon carbide

1. Introduction

Current developments in atomistic simulations for analyzing materials properties and behavior point to a capability which is potentially useful in materials design. Using many-body potential functions one can now investigate complex phenomena and processes at the atomistic level; moreover, the resulting atomic configurations can serve as inputs for the theoretically more rigorous approaches, such as tight binding approximation and first-principles calculations, also the calculated barrier energies can serve as parameters for mesoscopic level simulations such as kinetic Monte Carlo method which has a direct connection to experimental results.

In this way, simulation techniques which are appropriate on different length scales can be utilized collectively in a comprehensive analysis of how materials perform under service conditions. In this paper structural responses of covalent solids under an external stress have been investigated by molecular dynamics simulations where the unique capabilities provided by atomistic simulations for specific applications have been exploited.

2. Interatomic potential model

The empirical interatomic potential function developed by Tersoff [1] was employed in this study for both Si and SiC. Because the parameter values of the potential were determined to reproduce the elastic constants [1], the potential is more likely to be applicable for the analysis of deformation behavior. In dealing with a wide range of pressures (and therefore corresponding volume changes), we have observed undesirable interaction effects involving the second neighbors which arise from the short cutoff range of the potential. To avoid this effect, a modification is made by scaling the cutoff distance for the interaction range with the cube root of the system volume [2].

3. Elastic stability analysis

Recently, it has been demonstrated that the well-known elastic stability conditions [3] do not correctly describe the stability limits of crystals at finite strain, and the analysis of a deformed lattice stability requires the use of elastic

*Corresponding author.

[1]Present address: H-Division, Lawrence Livermore National Laboratory, Livermore, CA 94550, USA.

0925-8388/98/$19.00
PII: S0925-8388(98)00614-8

stiffness coefficients which are the generalization of elastic constants to finite strain. [4,5] The validity of the new criteria was tested for several problems of crystal deformation [4–10], also it has been discussed in a thermodynamic framework [11]. The newly derived stability criteria for cubic crystals under hydrostatic compression can be written as follows [4,5],

$$\tilde{B}_T = (C_{11} + 2C_{12} + P)/3 > 0 \quad (1)$$

$$\tilde{G} = C_{44} - P > 0 \quad (2)$$

$$\tilde{G}' = (C_{11} - C_{12})/2 - P > 0 \quad (3)$$

where $\tilde{B}_T$, $\tilde{G}'$ and $\tilde{G}$ may be regarded as the pressure-dependent bulk modulus, rhombohedral and tetragonal shear moduli respectively, and C are the conventional elastic constants in Voigt notation. We apply these criteria to analyze the elastic stability of Si and β-SiC under compression. The elastic constants C_{11}, C_{12}, and C_{44} at various states of compression were computed through fluctuation formula [12] at zero temperature and 300 K. Because the fluctuation formula cannot be used to obtain C_{44} at zero temperature [13], we also performed a stress–strain calculation while allowing for atomic relaxation within each unit cell.

In Fig. 1 it is clearly shown that values of $\tilde{G}'$ vanish at $r/r_0 = 0.893$ and 0.865, corresponding to pressures of 64 GPa (300 K) and 105 GPa (0 K) in the case of Si, also a value of G vanishes at r/r_0 of 0.734, corresponding to a pressure of 1156 GPa (0 K) in the case of Si. For SiC at 300 K, $\tilde{G}$ is found to also vanish at $r/r_0 = 0.775$, corresponding to pressures of 714 GPa. Thus, critical pressures at which the lattices become unstable under compression have been predicted.

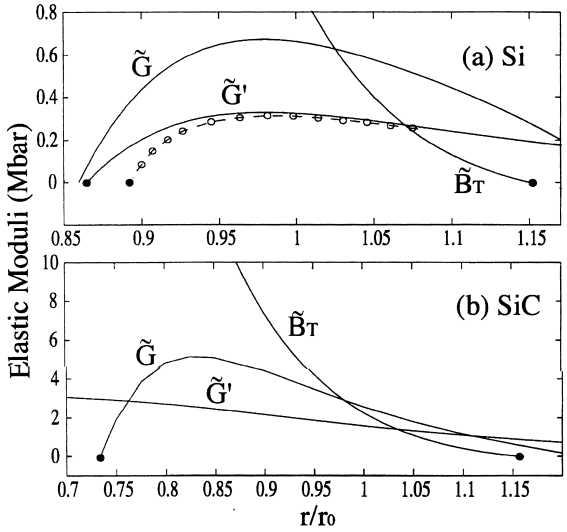

Fig. 1. Variations of elastic moduli with lattice parameter in Si (a) and SiC (b) at 0 K (curves) and 300 K (open circles); r and r_0 denote lattice parameters at current and zero pressure, respectively.

4. Molecular dynamics simulations

We next carried out molecular dynamics simulations to test the predictions of the elastic stability analysis. The simulation involved 216 atoms arranged in the diamond-cubic or zinc-blende structure for Si or SiC, respectively, with periodic boundary conditions and the lattice parameters set at the equilibrium values. The equations of motion were integrated by means of a predictor–corrector algorithm, and pressure was imposed by following the method of Parrinello and Rahman [14]. The system was first equilibrated at zero pressure, then pressure was incrementally increased with an equilibration period of 15 000–60 000 time steps (each step is 0.26–48 fs). All runs were made at a temperature of 300 K maintained by velocity rescaling at every time step.

In Fig. 2 the system volume and energy at various stages of compression obtained for Si is shown. An abrupt volume decrease is seen at 64 GPa, along with a corresponding energy reduction. In Fig. 3 the temporal evolution of volume, energy and the three diagonal elements of the simulation cell matrix h_{ij} [14] at the critical pressure of 64 GPa are shown. Here, a structural transformation is clearly observed at about time step 8000. The final structure obtained after the transformation is confirmed as a β-Sn structure by inspecting final atomic configuration. The results for SiC are shown in Figs. 4 and 5 with a static structure factor $s(k)$, evaluated for $k = (2\pi/a)(1,1,1)$. An abrupt change occurred at $P = 707$ GPa. One sees that $s(k)$ drops sharply to an essentially zero value, indicating a loss of structural order. Inspection of the final atomic configuration and other results of Figs. 4 and 5 signify that the abrupt change observed is a crystal-to-amorphous transition induced by compression. Here we note that the critical pressures observed in the molecular dynamics simulations are in close agreement with that predicted by the elastic

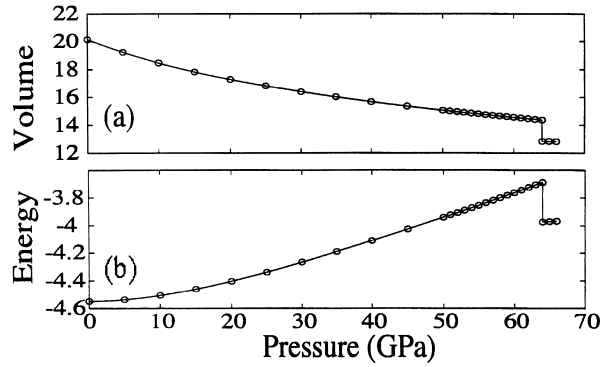

Fig. 2. System response of Si lattice at 300 K to compression as simulated by MD; (a) volume (Å^3/atom), (b) energy (eV/atom).

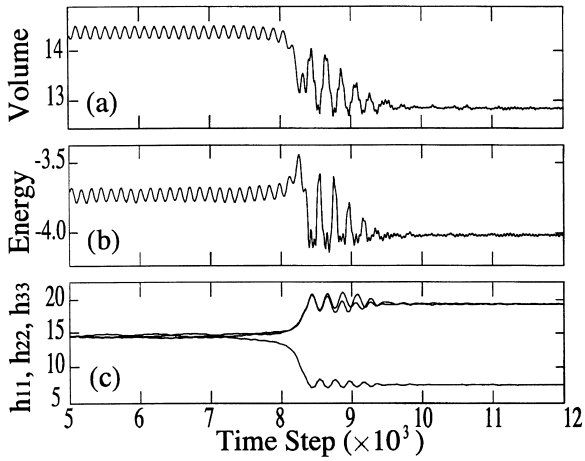

Fig. 3. Temporal behavior of Si lattice at critical pressure of 64 GPa as simulated by MD at 300 K; (a) volume (Å^3/atom), (b) energy (eV/atom), (c) diagonal elements of the cell matrix.

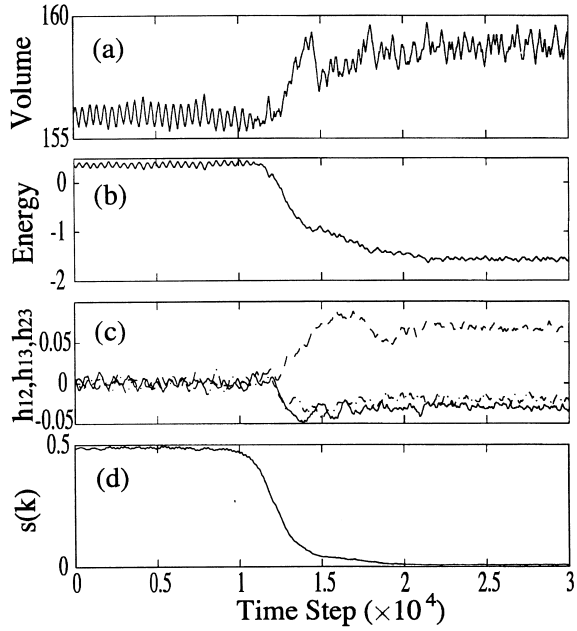

Fig. 5. Temporal behavior of SiC lattice at critical pressure of 714 GPa as simulated by MD at 300 K; (a) simulation cell volume in units of 6.538 Å^3, (b) energy (eV/atom), (c) off-diagonal elements of the cell matrix, (d) $s(k)$.

stability analysis in Fig. 1 for both Si and SiC. Thus, the predictions of critical pressures are verified by molecular dynamics simulations.

5. Activation barrier against homogeneous deformation

Conventional theoretical prediction of transition pressure between two structures tends to be a determination of the cohesive energy curves from which the critical pressure is obtained by a common tangent construction. This analysis is based on the thermodynamic requirement of equality of free energies at zero temperature [15,16]. According to thermodynamics, two phases coexist at a pressure where the Gibbs free energies, $G=E+PV-TS$, of the two structures are equal. At zero temperature. the only information needed to determine the transition pressure is the energy variation with volume, since pressure is given by the identity $P=\partial E/\partial V$. Applying this analysis ab initio calculations predicted consistent values [15,16,7] with

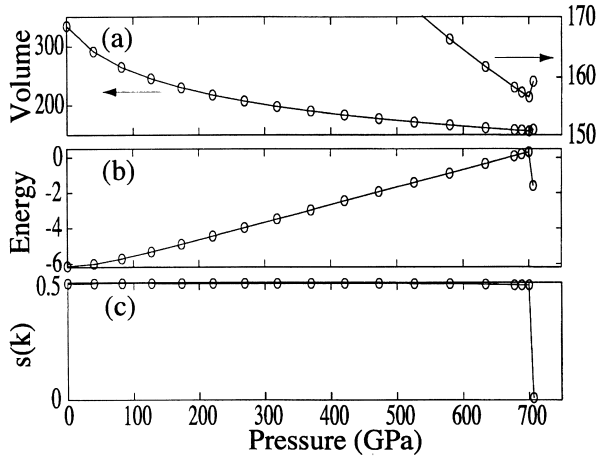

Fig. 4. System responses of SiC lattice at 300 K to compression as simulated by MD; (a) simulation cell volume in units of 6.538 Å^3, (b) energy (eV/atom), (c) static structure factor.

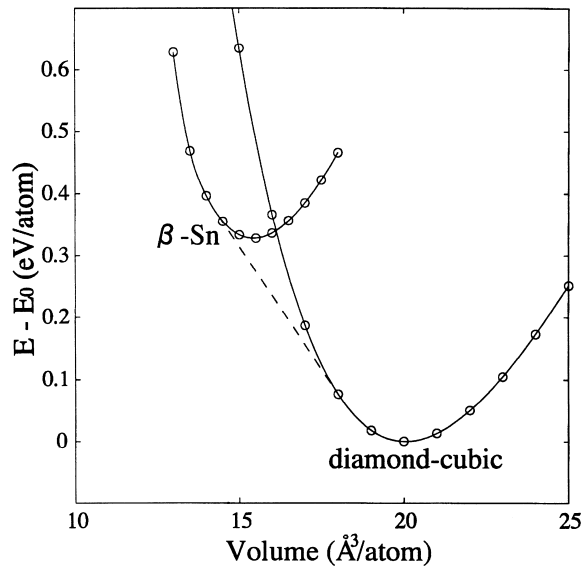

Fig. 6. Energy vs volume relation for Si in the diamond-cubic and β-Sn structures.

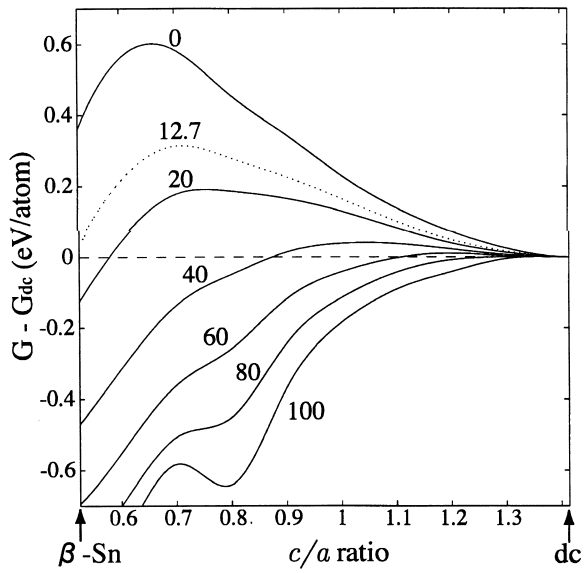

Fig. 7. Curves of free energy at 0 K along a reaction path of homogeneous deformation. Numbers denote pressures in GPa.

experimental values reported as 8.8 to 12.5 GPa [17,18] for Si.

For the case of Si, we applied the thermodynamic criteria to the Tersoff potential to obtain a transition pressure of 12.7 GPa at zero temperature, as shown in Fig. 6. This predicted value is consistent with experiments too, but considerably lower than that obtained by the elastic stability analysis and the molecular dynamics simulation. This apparent discrepancy stems from the existence of an activation barrier between the two structures.

In order to verify the activation barrier at zero temperature, we prepared a series of intermediate lattice structures which have c/a ratios between the limiting values of $\sqrt{2}$ (diamond-cubic) and 0.524 (β-Sn). For each of these lattices we calculated the energy and pressure at several values of atomic volume. The activation barrier in the sense of homogeneous deformation along a reaction coordinate identified with the c/a ratio can be displayed explicitly in Fig. 7 by converting the results to energy variations with c/a ratio at fixed pressures. The barrier height, 0.6 eV/atom at zero pressure, is seen to decrease with increasing pressure and vanishes at around 80 GPa. The obtained activation energy at the critical pressure of 12.7 GPa, according to the thermodynamics criteria, is about 0.3 eV/atom in Fig. 7.

Thus, existence of an activation barrier is shown, and we suggest that the critical pressures obtained by the elastic stability criteria and the molecular dynamics are the upper bound of crystal stability corresponding to the homogeneous transformation path over the barrier, in contrast, the transition pressure obtained by the thermodynamic criteria is the lower bound corresponding to the barrierless transition. Concerning the experimental observations [17,18], we believe that experimental values are close to the lower bound because the barrier effects can be decreased, apparently due to the existence of defects.

6. A mechanism of amorphization

In contrast to the polymorphic transition of Si, β-SiC is found to undergo an amorphization under pressure in molecular dynamics simulations. We examined energy vs volume relations for SiC in the zinc-blende, rocksalt and β-Sn structures which are believed to be relevant structures of crystalline SiC under high pressure. We found that free energy at zero temperature for β-Sn structure is always higher than that for zinc-blende structure. This means that no transition from zinc-blende to β-Sn is expected under compression. On the other hand, for the rocksalt structure, we did find a transition pressure of 649 GPa at zero temperature. Since the transition pressure we obtained in molecular dynamics simulations for SiC (707 GPa) was higher than that for rocksalt structure, the amorphous phase we obtained in molecular dynamics simulations is likely to be a metastable phase.

We next investigated the underlying role of the different structural responses between Si and SiC by considering the two effects associated with chemical ordering in β-SiC, a difference in the atomic sizes of C and Si, and the chemical preference of Si(C) to have the other species as its nearest neighbors. To separate the effects of size disparity from that of mixed bond preference, we note that the Tersoff potential is of the form $V_{ij} f_c(r_{ij})[A_{ij} e^{\lambda_{ij} r_j} - B_{ij} \chi b_{ij}] e^{-\mu_{ij} r_j}$, where the two effects are described through the bond order parameter b_{ij} and the factor χ, respectively [1]. Since $\chi = 1$ when i and j refer to atoms of the same species, its value affects only V_{Si-C} and V_{C-j}, and therefore the heat of formation ΔH. On the other hand, to suppress the effect of atomic size difference, one can simply set $b_{C-j} = b_{Si-j}$ in functional form. This observation leads us to examine two idealizations of the Tersoff potential; one in which mixed bond preference is suppressed through adjusting χ to give $\Delta H = 0$ (model I), and another in which size difference is suppressed by the method just described while at the same time adjust χ so that ΔH remains unchanged (model II).

In Table 1 the elastic constants, the lattice parameter, and the cohesive energy calculated for the two idealized models at equilibrium configuration and 0 K are compared with values for the full model. It is clearly seen that while the elimination of chemical bond preference has little effect on the elastic constants, all three elastic constants are significantly altered in the absence of atomic size difference. Although both $(C_{11}-C_{12})$ and C_{44} are appreciably reduced, the lowering of the former is more drastic such that in model II the elastic instability is found to be the vanishing of $\tilde{G}'$. This result is consistent with the behavior obtained in the case of Si in Fig. 2. Thus, we have shown

Table 1
Comparison of properties calculated using the Tersoff potential and the two idealizations, models I and II

	Tersoff	Model I	Model II
Lattice parameter	4.32	4.34	4.32
Cohesive energy [eV]	−6.19	−6.03	−6.19
Bulk modulus [Mbar]	2.25	2.18	2.25
C_{11} [Mbar]	4.36	4.19	3.31
C_{12}	1.20	1.17	1.72
C_{44}	2.56	2.42	1.61
$C_{11}-C_{12}$	3.16	3.02	1.59

that the difference between SiC and Si in compression-induced structural response lies in the dominant role of atomic size effect. In other words, amorphization occurs in SiC because the onset of vanishing of $\tilde{G}$ precludes a polymorphic transition associated with the instability of $\tilde{G}'=0$. To demonstrate that this is the correct interpretation, we have carried out a simulation of model II under compression and indeed observed a transition from zinc-blende to rock salt structure which is triggered by the tetragonal shear instability.

7. A perspective on materials design

We have presented specific results which elucidate the physical mechanisms of structural response to external stress in covalent crystals. Clearly, the usefulness of this type of atomic-level simulation depends on accuracy of the potential function model. For the analysis to be predictive and play a central role in the holistic process of materials design, it will be necessary to integrate atomistic simulations with ab initio electronic structure methods on the one hand, and with mesoscopic simulations capable of treating micron-size length scales on the other. There is increasing recognition that such a multiscale modelling approach is essential if one is to realize the full potentials of molecular engineering of technological materials [19].

Acknowledgements

We acknowledge helpful discussions with J. Wang.

References

[1] J. Tersoff, Phys. Rev. B 38 (1988) 9902.
[2] M. Tang, S. Yip, Phys. Rev. B 52 (1995) 15150.
[3] M. Born, K. Huang, Dynamical Theory of Crystal Lattices, Clarendon, Oxford, 1956.
[4] J. Wang, S. Yip, S.R. Phillpot, D.W. Wolf, Phys. Rev. Lett. 71 (1993) 4182.
[5] J. Wang, J. Li, S. Yip, S.R. Phillpot, D. Walf, Phys. Rev. B 52 (1995) 12627.
[6] M. Tang, S. Yip, J. Appl. Phys. 76 (1994) 2719.
[7] K. Mizushima, S. Yip, B. Kaxiras, Phys. Rev. B 50 (1994) 14952.
[8] F. Cleri, J. Wang, S. Yip, J. Appl. Phys. 77 (1995) 1449.
[9] M. Tang, S. Yip, Phys. Rev. Lett. 75 (1995) 2738.
[10] M. Celino, F. Cleri, G. DAgostino, V. Rosato, Phys. Rev. Lett. 77 (1996) 2495.
[11] Z. Zhou, B. Joós, Phys. Rev. B 54 (1996) 3841.
[12] M.D. Kluge, J.R. Ray, A. Rahman, J. Chem. Phys. 85 (1986) 4026.
[13] J.R. Ray, Comp. Phys. Repts. 8 (1988) 109.
[14] M. Parrinello, A. Rahman, J. Appl. Phys. 52 (1981) 7182.
[15] M.T. Yin, M.L. Cohen, Phys. Rev. Lett. 45 (1980) 1004.
[16] M.T. Yin, M.L. Cohen, Phys. Rev. Lett. 4526 (1982) 5668.
[17] H. Olijnyk, S.K. Sikka, W.B. Holzapfel, Phys. Lett. 103A (1984) 137.
[18] J.Z. Hu, L.D. Merkel, C.S. Menoni, I.L. Spain, Phys. Rev. B 34 (1989) 4679.
[19] See the Proceedings of the Workshop on Modelling of Industrial Materials: Connecting Atomistic and Continuum Scales, January 1996, UC Santa Barbara, published in J. Computer-Aided Materials Design, Vol._3, 1996.